Mitigating Drought Conditions under Climate and Land Use Changes by Applying Hedging Rules for the Multi-Reservoir System

Zejun Li [1,2,3,4,*] , Bensheng Huang [2,3,4], Zhifeng Yang [1], Jing Qiu [2,3,4], Bikui Zhao [2,3,4] and Yanpeng Cai [1]

1   Institute of Environmental & Ecological Engineering, Guangdong University of Technology, Guangzhou 510006, China; zfyang@gdut.edu.cn (Z.Y.); yanpeng.cai@gdut.edu.cn (Y.C.)
2   Guangdong Research Institute of Water Resources and Hydropower, Guangzhou 510635, China; bensheng@21cn.com (B.H.); jingqiusks@sina.com (J.Q.); zbk0615@163.com (B.Z.)
3   National and Local Joint Engineering Laboratory of Estuarine Water Technology, Guangzhou 510635, China
4   Southern Marine Science and Engineering Guangdong Laboratory (Zhuhai), Zhuhai 519082, China
*   Correspondence: lizejun09@163.com; Tel.: +86-185-9405-0819

Abstract: Climate and land use changes have substantially affected hydrologic cycles and increased the risk of drought. Reservoirs are one of the important means to provide resilience against hydrologic variability and achieve sustainable water management. Therefore, adaptive reservoir operating rules are needed to mitigate their adverse effects. In this study, the Hanjiang River Basin in southeast China was selected as the study area. Future climate and land use projections were produced by the Delta method and CA-Markov model, respectively. Future climate forcings and land use patterns were then incorporated into a distributed hydrologic model to evaluate river flow regime shifts. Results revealed that climate and land use changes may lead to severe drought conditions in the future. Lower flows are shown to be more sensitive to environmental changes and a decline of monthly flows could reach up to nearly 30% in the dry season. To address the threat of increasing drought uncertainties in the water supply system, the aggregation-decomposition method incorporated with hedging rules was applied to guide the multi-reservoir operation. Parameters of optimal hedging rules were obtained by a multi-objective optimization algorithm. The performance of hedging rules was evaluated by comparison to standard operating policies and conventional operating rules with respect to reliability, resiliency, vulnerability, and sustainability indices. Results showed that the multi-reservoir system guided by hedging rules can be more adaptive to the environmental changes.

Keywords: climate and land use changes; SWAT model; hedging rules; aggregation-decomposition; drought conditions

1. Introduction

Water has been widely perceived as one of the most important natural resources to sustain human social and economic development. Water conservancy projects and water supply systems are designed to meet anthropogenic and environmental water needs [1]. However, the intensification of human activities over the past century has dramatically accelerated the global land use and climate change rate, and changes are certain to continue in the near future. In the context of changing environments, the water supply system, which has been designed based on the original characteristics of water resources, may face more challenges to adapt to hydrological regime shifts.

Climate and land use changes have substantially affected terrestrial hydrological cycles. Increased greenhouse gas emissions lead to a rise in air temperature, and thus, intensify the terrestrial hydrological cycle, causing more extreme hydrometeorological events. Middelkoop et al. [2] revealed that climate change will lead to higher winter flow and lower summer flow in the Rhine basin. The shifts of flow regime would put pressure

on local water security and water availability. Xu et al. [3] exhibited a decline of river runoff in winter, while an increase in summer under all of the emission scenarios, implying more possible extreme disasters (floods and droughts) may appear in Qiantang River Basin, East China. In contrast with climate change, land use changes usually affect the water distribution on the land surface through processes such as interception, infiltration, surface/subsurface runoff, and evapotranspiration, etc. For example, urbanization expands the impervious surface area, which will reduce infiltration and the concentration time. Therefore, urbanization may come with more flash floods with higher peaks [4,5]. Evapotranspiration is usually more sensitive when regional dominant land cover conversions take place [6,7]. Moreover, previous studies investigated the combined effect of land use and climate change on water resources. A large number of these studies discovered that the frequency and intensity of future floods and droughts would become more unprecedented under the changing environments [8,9].

Reservoirs are one of the important means to provide resilience against hydrologic variability and achieve sustainable water management [10–12]. However, the hydrological flow regime shifts in the future may pose big challenges for the reservoir design and operation under the assumption of hydrologic stationarity [13,14]. For example, Georgakakos et al. [15] pointed out that current reservoir operation policies would be incompetent to satisfy the water supply needs during drought periods under climate change. Therefore, it is necessary to improve the adaptability, reliability, and resilience of existing reservoir systems under the increasing environmental uncertainties [16].

To mitigate the impacts of climate and land use changes, a number of adaptive reservoir operating policies have been proposed. Specifically, the hedging mechanism has been wildly applied to cope with the increasing uncertainties of future flow patterns. Compared with the standard operating policies (SOPs), which release water as close to the water demand as possible, only saving a surplus of water for future use, the hedging rules (HRs) would accept small deficits in the current stage to reduce the probability of a severe water shortage later [17–19]. Therefore, HRs tend to be more resilient to the flow regime changes that are intensified by the changing environments. Steinschneider et al. [20] developed an adaptation strategy by combining hydrologic forecast information and risk hedging via an option instrument. Results suggested that the proposed strategy could effectively improve system reliability under climate change scenarios. In order to alleviate the damage of future droughts, Karamouz et al. [21] applied hedging rules into the contingency planning scheme of the reservoir to reduce the damages of water deficit. Adeloye et al. [22] developed optimized static and dynamic zone based hedging policies for reservoir operation, which could better utilize the buffering capacity to reduce the system vulnerability. Alimohammadi et al. [23] changed the SOP into a Modified Linear Decision Rule policy, which avoided the complete draining of the reservoir for several consecutive months by giving agricultural demands a lower priority than the urban water supply. Ahmadianfar et al. [24] introduced a two-dimensional hedging policy into the agricultural reservoir operation, revealing decreased vulnerability and water deficit under the RCP 8.5 climate scenario.

Even though HRs have been proven to be an effective way to cope with the uncertainties of future drought, few studies made efforts to investigate how to derive adaptive joint operating rules based on HRs for the multi-reservoir water supply system under the changing environments. For a multi-reservoir system, the cooperation for reservoirs is needed to achieve optimal water resources management. The aggregation-decomposition method has been proven to be one of the effective ways [25–27]. The basic idea of the multi-reservoir aggregation-decomposition method is to aggregate multiple reservoirs into a virtual aggregated reservoir to determine the optimal total output, which is then allocated to individual reservoirs [28,29].

This paper aimed at investigating the impact of climate and land use changes on drought conditions, and then proposed the adaptive operating rules for the multi-reservoir system. The Hanjiang River Basin in southeastern China was selected as the study area,

where the lack of enough reservoir regulation capacity together with the large amount of anthropogenic water demand make the water supply system more vulnerable to streamflow uncertainties. Based on the Bureau of Hydrology and Water Resources Pearl River Water Resources Commission of Ministry of Water Resources in China, the monthly average runoff of the Hanjiang River Basin was down 20%–90% from the historical average for 25 consecutive months from 2019 to 2021, due to climatic anomaly, which led to the most severe drought conditions since 1956. Therefore, a deeper understanding of the adaptive management is expected to contribute to drought mitigation under climate and land use changes. The remainder of this paper is organized as follows. The methodology is introduced in Section 2. Section 3 introduces the study area and the data used in this study. Subsequently, the results and discussion are presented in Section 4. The conclusions are drawn in Section 5.

2. Methodology

The flowchart of this study consists of two main parts, and it has been shown in Figure 1: (1) Evaluation of low flow regime changes, which is based on land use projection, climate change projection, and SWAT model simulation; (2) evaluation of reservoir operation performance by comparing adaptive hedging rules with standard operating rules and conventional operating rules.
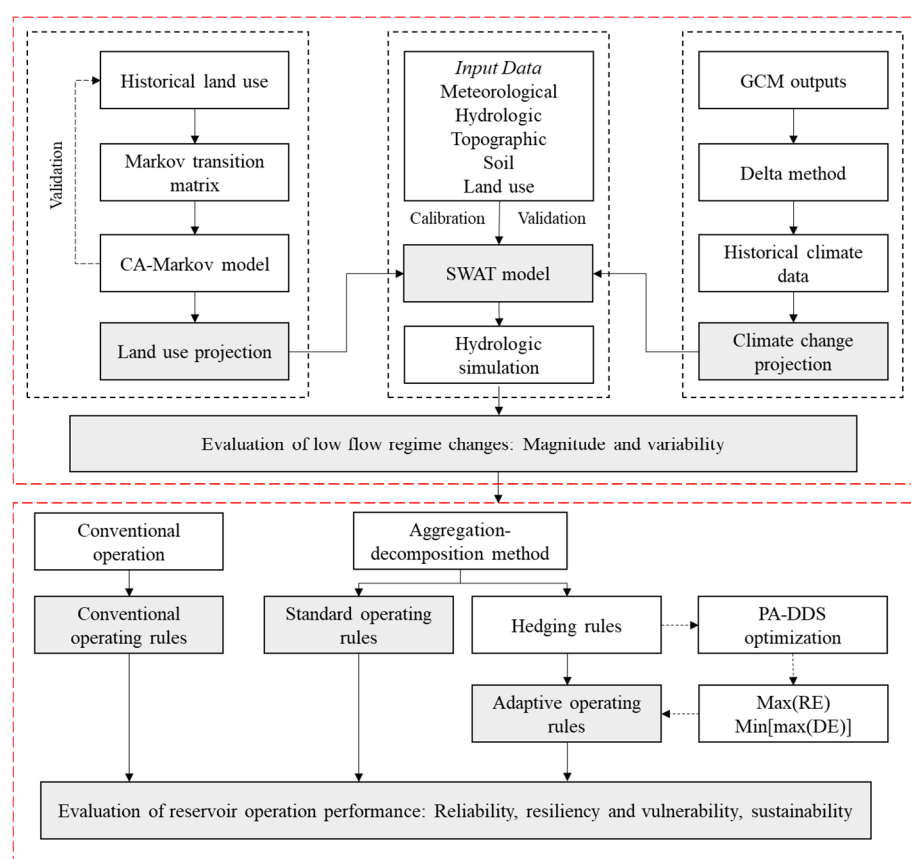

Figure 1. Flowchart of the methodology.

2.1. Hydrologic Model

The soil and water assessment tool (SWAT) model is a physically based, continuous-time, distributed parameter model that is able to simulate the quality and quantity of water on the basin scale and predict the impact of land use and climate changes [30,31]. The hydrologic routines in the SWAT model consist of the following components: Weather, surface/subsurface runoff, groundwater flow, percolation, evapotranspiration, reach routing,

etc. The SWAT model applies a two-level spatial discretization scheme. Specifically, the watershed is first divided into sub-basins based on topography and further discretized into hydrologic response units (HRUs), with the homogeneous land use, soil type, topography, and management approach [32].

The sequential uncertainty fitting version 2 (SUFI-2) program, embedded in the SWAT-CUP (calibration and uncertainty procedures) [33] was utilized in the model calibration. The SWAT-CUP is able to calibrate model parameters in different spatial scales, including the basin, sub-basin, and HRU scales.

2.2. Land Use Projections

In this study, the CA–Markov model, embedded in IDRISI Selva, was used to produce land use projections. Cellular automata (CA) is a dynamic process model with powerful spatial computing ability. The Markov process refers to a random process, whose future probabilities are determined by its most recent values. The CA–Markov model combines the advantages of these two processes, and can be used to carry out the spatial–temporal land use change simulation [34]. The CA–Markov model iteratively simulates the spatial distribution of land use based on the Markov transition matrix and transition suitability image. The Kappa index is commonly used to evaluate the land use simulation results [35]. A Kappa index value greater than 0.75 denotes a decent consistency of two land use maps. The Kappa index is defined as follows:

$$Kappa = \frac{P_0 - P_c}{P_p - P_c} \qquad (1)$$

where P_0 is the percent correct for the output; P_c is the expected percent correct due to change; and P_p is the percent correct when the classification is perfect.

The following example illustrates the approach to make land use projections. Given the land use maps of 1995, 2010, and 2015, in order to produce the land use patterns in 2050, there will be three steps: (1) Based on land use maps of the year 1995 and 2010, IDRISI Selva calculates the Markov transition matrix, taking 1 year as the time step. (2) Taking the land use map of 1995 as the initial state, the CA-Markov model simulates the land use variation iteratively and finally the land use map of 2015 is generated. The Kappa index was calculated to validate the simulation results. (3) On the basis of decent model performance in step (2), the CA-Markov model can be applied to simulate the land use map of 2050 starting from 2015.

2.3. Climate Change Projections

In this study, the Delta method was used to generate precipitation and temperature data series under future climate scenarios. The basic theory of the Delta method is to scale the observed climate according to the simulated changes, which are derived from GCMs [36,37]. To this aim, the monthly average differences of climatic variables (temperature and precipitation), extracted from the GCM output, between future and historical periods were first calculated. Then, the differences were superimposed to the baseline climate data series. The differences of monthly mean temperature ΔT_i and the ratio of monthly mean precipitation ΔP_i were calculated based on:

$$\Delta T_i = (\overline{T}_{fut,i} - \overline{T}_{base,i}) \qquad (2)$$

$$\Delta P_i = \overline{P}_{fut,i} / \overline{P}_{base,i} \qquad (3)$$

where $\overline{T}_{fut,i}$ and $\overline{T}_{base,i}$ are the average temperature of GCM for the ith month in future and baseline time periods, respectively. $\overline{P}_{fut,i}$ and $\overline{P}_{base,i}$ are the average precipitation amount of GCM for the ith month in future and baseline time periods, respectively.

2.4. Multi-Reservoir Operation Model

2.4.1. Aggregation-Decomposition Method

The aggregation-decomposition method was used in the multi-reservoir operation. Reservoirs were aggregated in the unit of water volume and then decomposed based on the percentage of inflow. The reservoirs can be aggregated as follows:

$$V(t) = \sum_{j=1}^{N} \left[V_j(t) + I_j(t) \times \Delta t \right] \tag{4}$$

where $V(t)$ is the storage of the aggregated virtual reservoir at the beginning of time period t; $V_j(t)$ is the storage of reservoir j at the beginning of time period t; $I_j(t)$ is the inflow of reservoir j during time period t; Δt is the time interval; and N is the number of reservoirs.

Hedging rules (HRs) were applied as the operating rules for the virtual aggregated reservoir operation. SOPs were applied as the baseline for comparison. The SOPs and HRs of the aggregated reservoir are shown in Figure 2.
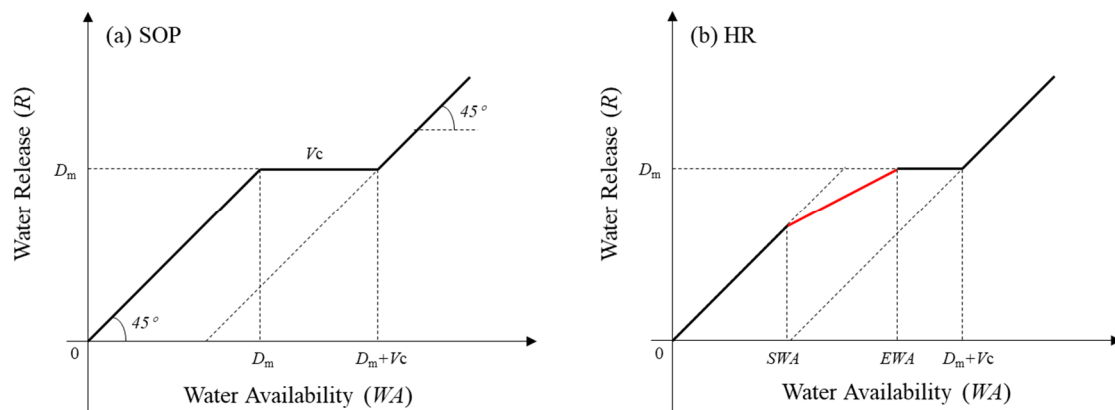

Figure 2. Operation rules of the aggregated reservoir: (**a**) SOP; (**b**) HR. D_m refers to the water demand, and V_c refers to the active capacity of the reservoir.

As seen in Figure 2b, the two-point hedging rule contains two parameters, *SWA* and *EWA*, representing the starting and ending water availability for hedging, respectively. The water release of the virtual aggregated reservoir could be calculated using Equation (5), as shown below:

$$R_t = \begin{cases} WA_t & WA_t < SWA_t \\ D_t + (SWA_t - D_t)\frac{WA_t - EWA_t}{SWA_t - EWA_t} & SWA_t \leq WA_t \leq EWA_t \\ D_t & EWA_t \leq WA_t < D_t + V_c \\ WA_t - V_c & WA_t \geq D_t + V_c \end{cases} \tag{5}$$

where t denotes the time period.

The total release R_t calculated using Equation (5) could then be allocated to the individual reservoirs using Equation (6), as shown below:

$$R_j(t) = R(t) \times \frac{I_j(t)}{\sum_{j=1}^{N} I_j(t)} \tag{6}$$

where $R_j(t)$ is the water release of individual reservoir j during the time period t; and $I_j(t)$ is the inflow of individual reservoir j during the time period t.

The constraints considered in the model include water balance, water storage limits, and release capacity, as shown below:

$$V_j(t+1) = V_j(t) + (I_j(t) - R_j(t))\Delta t \tag{7}$$

$$V_{j,min} \leq V_j(t) \leq V_{j,max} \tag{8}$$

$$R_{j,min} \leq R_j(t) \leq R_{j,max} \tag{9}$$

where $V_j(t)$ and $V_j(t+1)$ are the beginning and ending storage limits of reservoir j at time period t; $V_{j,\min}$ and $V_{j,\max}$ are the lower and upper water storage limits of reservoir j; and $R_{j,\min}$ and $R_{j,\max}$ are the lower and upper water release limits of reservoir j.

2.4.2. Optimization Method

Two objective functions were selected to evaluate the multi-reservoir operation model performance, which are to maximize the water supply reliability (*RE*) and to minimize the maximum water deficit (*DE*).

$$max(RE) \Leftrightarrow max\left\{ \frac{\sum_{t=1}^{T} Z(t)}{T} \right\} \times 100\% \tag{10}$$

$$min(DE) \Leftrightarrow min\left\{ max\left(1 - \frac{Q(t)}{D_m}\right) \right\} \times 100\% \tag{11}$$

where $Z(t)$ is a binary indicator. When the flow $Q(t)$ is greater than the water demand D_m at the cross section, $Z(t)$ is equal to 1. Otherwise, $Z(t)$ is equal to 0.

The HRs were optimized through the Pareto-archived dynamically dimensioned search (PA-DDS) algorithm [38]. PA-DDS is a multi-objective optimization algorithm, which has shown its efficiency and effectiveness in solving water resources problems in previous studies [39–41].

2.5. Evaluation Indicators

(1.) Hydrologic model performance

The Nash-Sutcliffe efficiency (*NSE*), relative error (*RE*), and coefficient of determination (R^2) were used to evaluate the SWAT model performance, which can be defined as:

$$NSE = 1 - \frac{\sum_{t=1}^{T}(Q_{s,t} - Q_{o,t})^2}{\sum_{t=1}^{T}(Q_{o,t} - \overline{Q_o})^2} \tag{12}$$

$$RE = \frac{|\sum_{t=1}^{T} Q_{o,t} - \sum_{t=1}^{T} Q_{s,t}|}{\sum_{t=1}^{T} Q_{o,t}} \times 100\% \tag{13}$$

$$R^2 = \frac{[\sum_{t=1}^{T}(Q_{o,t} - \overline{Q_o})(Q_{s,t} - \overline{Q_s})]^2}{\sum_{t=1}^{T}(Q_{o,t} - \overline{Q_o})^2 \sum_{t=1}^{T}(Q_{s,t} - \overline{Q_s})^2} \tag{14}$$

where $Q_{s,t}$ and $Q_{o,t}$ refer to the simulated and observed streamflow at time period t, respectively. $\overline{Q_s}$ and $\overline{Q_o}$ refer to the mean of simulated and observed streamflow, respectively.

(2.) Regime changes

To evaluate the regime changes of low flow under changing environments, indicators were selected from the perspective of magnitude and variability [42]. The three selected magnitude indicators are the 90th percentile of daily flow (Q_{90}), the lowest seven consecutive average flow (Q_{min7}), and the average flow ($\overline{Q}$). Q_{90} is a robust indicator of low flows; Q_{min7} indicates consecutive extreme low flows; and $\overline{Q}$ represents the average amount of water. One selected variability indicator is the interquartile range between Q_{50} and Q_{90} (Q_{var}), which represents the variation of low flows.

(3.) Reservoir operation performance

Reliability, resiliency, and vulnerability indices were introduced to evaluate the performance of the reservoir operation system in the Hanjiang River Basin. Reliability has been defined in Section 2.4.2, and here denoted by I_{RE}. The resilience index (I_{RS}) is used to measure the recovery rate from an unsatisfactory state [43,44], which can be defined as follows:

$$I_{RS} = \frac{\sum_{t=1}^{T-1} W(t)}{T - \sum_{t=1}^{T} Z(t)} \tag{15}$$

where $W(t)$ is a binary indicator. If $Z(t) = 0$ and $Z(t+1) = 1$, then $W(t) = 1$. Otherwise $W(t) = 0$. Vulnerability is represented by the mean water deficit, and here denoted by I_{VU}. Finally, a sustainability index (I_S) was introduced to represent the combined performance of the above three indices [24], which can be defined as follows:

$$I_S = [I_{RE} \times I_{RS} \times (1 - I_{VU})]^{\frac{1}{3}} \tag{16}$$

3. Case Study

3.1. Study Area

The Hanjiang River is one of the most important rivers in southeast China. It lies between 23.28 and 26.08° N and between 115.22 and 117.2° E, with an area of 30,112 km². The Hanjiang River Basin spans three provinces (Guangdong, Fujian, and Jiangxi), and around 10.7 million people live there. The Hanjiang River Basin has a subtropical climate and the annual average precipitation in this basin is around 1600 mm, but its temporal distribution is uneven, with the amount in the flood season accounting for almost 80%. On the other hand, compared with the average annual total anthropogenic water use in the basin (4.5 billion m³), the total active storage of the large reservoirs is only 1.4 billion m³, which indicates a relatively weak water regulation capacity.

The Tingjiang River and the Meijiang River are the two main tributaries. As shown in Figure 3, there are five large reservoirs in the Hanjiang River Basin, with Mianhuatan Reservoir (MHT) located on the Tingjiang River and Changtan Reservoir (CT). The Heshui Reservoir (HS) and Yitang Reservoir (YT) are located on the tributaries of the Meijiang River. The Gaobei (GB) Reservoir is located on the mainstream of the Hanjiang River. The basic parameters of reservoirs are listed in Table 1.
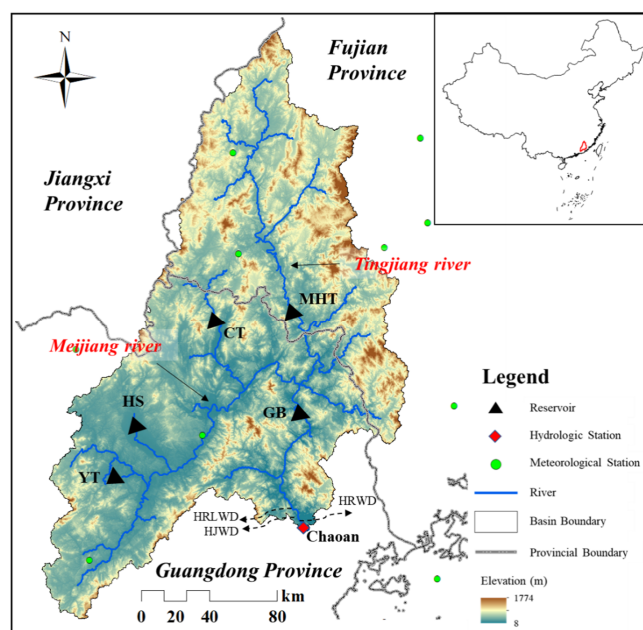

Figure 3. Profile of Hanjiang River Basin.

Table 1. Basic parameters of the reservoirs in Hanjiang River Basin.

	MHT	CT	HS	YT	GB
Catchment area (km^2)	7907	1990	251	578	26,590
Normal water level (m)	173	148	138	153	38
Dead water level (m)	146	136.5	132.5	133	28
Active storage (10^6 m^3)	1122	54.5	41.3	107	93.9
Total storage (10^6 m^3)	2035	172	116	166	365.6

There are three water diversion projects in the basin, which are the Hanjiang-Rongjiang-Lianjiang water diversion project (HRLWD), Hanjiang-to-Jieyang water diversion project (HJWD), and Hanjiang-to-Raoping water diversion project (HRWD). Their maximum intake flows are 30, 11.3, and 4.6 m^3/s, respectively. All of the three water diversion projects take water from the river segment, which is at the upstream of the Chaoan hydrologic station.

3.2. Data

(1.)　Climate data

The daily climate data (including precipitation, air temperature, wind speed, radiation, and relative humidity) at 16 meteorological stations during the period from 1979 to 2005 were collected from the China Meteorological Data Sharing Service System.

A set of 23 general circulation models (GCMs), such as ACCESS1.0, BCC_CSM1.1, BNU-ESM, CanESM2, etc. derived from the fifth assessment report (AR5) of the intergovernmental panel on climate change (IPCC), were used to generate the climate projections data under climate change scenarios for both representative concentration pathways (RCP) 4.5 and 8.5. This study used the ensemble mean values of precipitation and air temperature to represent climate change projections, in order to reduce the uncertainties of the GCM models.

In this study, the baseline time period is from 1979 to 2005, and the future time period is from 2035 to 2060 (2050s).

(2.)　Streamflow data

The observed daily streamflow data during the period from 1979 to 2005 at Chaoan hydrologic station were collected from the Hydrology Bureau of Guangdong Province. The Chaoan hydrologic station was located on the control cross section of the lower reaches of the Hanjiang River Basin (Figure 1).

Streamflow data from 1979 to 1995 were used to calibrate the SWAT model (the first year serving as a warmup period) and data from 1996 to 2005 were used for validation.

(3.)　Topographic, soil data, land use/cover

The topography data were determined on the basis of the NASA shuttle radar topographic mission (SRTM) digital elevation model (DEM) with a cell size of 90 m × 90 m. A digital soil map was generated from the 1:1,000,000 scale soil map of China. Digital land cover/land use maps of the year 1995, 2010, and 2015 were derived from the large-scale (1: 100,000) land use map of China. They were regenerated by reclassifying into five main land use types (woodland, grassland, developed, agriculture, and water) in this study.

3.3. Reservoir Operation System

(1.)　Reservoirs

In the Hanjiang River Basin, the MHT, CT, HS, and YT reservoirs are in parallel and all of their water release will enter the GB reservoir in the downstream. In this study, four upstream parallel reservoirs were aggregated as a virtual reservoir. Therefore, the multi-reservoir system in the Hanjiang River Basin could be simplified as a cascade reservoir system comprised of two reservoirs.

The HRs were applied as the operating rules for both the aggregated virtual reservoir and GB reservoir in the downstream. There are two parameters (i.e., *SWA* and *EWA*)

for each reservoir. The time varying HRs were applied at monthly steps considering the uneven distribution of runoff throughout the year. Therefore, there are 48 parameters in total for the multi-reservoir system in the Hanjiang River Basin.

As a comparison scheme, the SOP rules were applied for the aggregated virtual reservoir and GB reservoir, as well as to investigate whether the system performance could be improved by HRs or not. Moreover, conventional operating rules (COs) of reservoirs were evaluated as the benchmark.

(2.)   Water diversion projects

Both HJWD and HRWD are designed for domestic water use. Therefore, the two projects take water from Hanjiang on the scale of 15.9 m^3/s, on a constant basis. In contrast with HJWD and HRWD, the HRLWD is designed to improve the aquatic ecosystem in other districts. Therefore, the HRLWD operates on the basis that the priority of flow at the Chaoan section was required to be guaranteed at first. The designed operation rules of HRLWD are: When the flow at the Chaoan section is less than 300 m^3/s, the project stops working. When the flow at the Chaoan section is larger than 300 m^3/s, the water intake of the project should not be larger than 30 m^3/s, guaranteeing a minimum flow at the Chaoan section that is not less than 300 m^3/s.

(3.)   Water demand at the Chaoan section

The Chaoan section is the controlling section of Hanjiang River Basin, where the downstream is the Hanjiang Delta region. The minimum environmental flow required at the Chaoan section is 128 m^3/s. However, the minimum discharge at the Chaoan section should not be lower than 180 m^3/s to meet the water demand in the Hanjiang Delta region. Therefore, the aim of reservoir operation is to guarantee the minimum discharge of 180 m^3/s at the Chaoan section.

4. Results and Discussion

4.1. Hydrologic Model Calibration and Validation

Figure 4 shows the calibration and validation results of the SWAT model. To help visualize the hydrograph, only the time periods from 1991 to 1998 are displayed. Results of evaluation indicators are listed in Table 2. Both in the calibration and validation periods, *NSE* values are higher than 0.7, *RE* are within 10%, and R^2 are higher than 0.7. The overall performance of the SWAT model constructed in Hanjiang River Basin is acceptable.
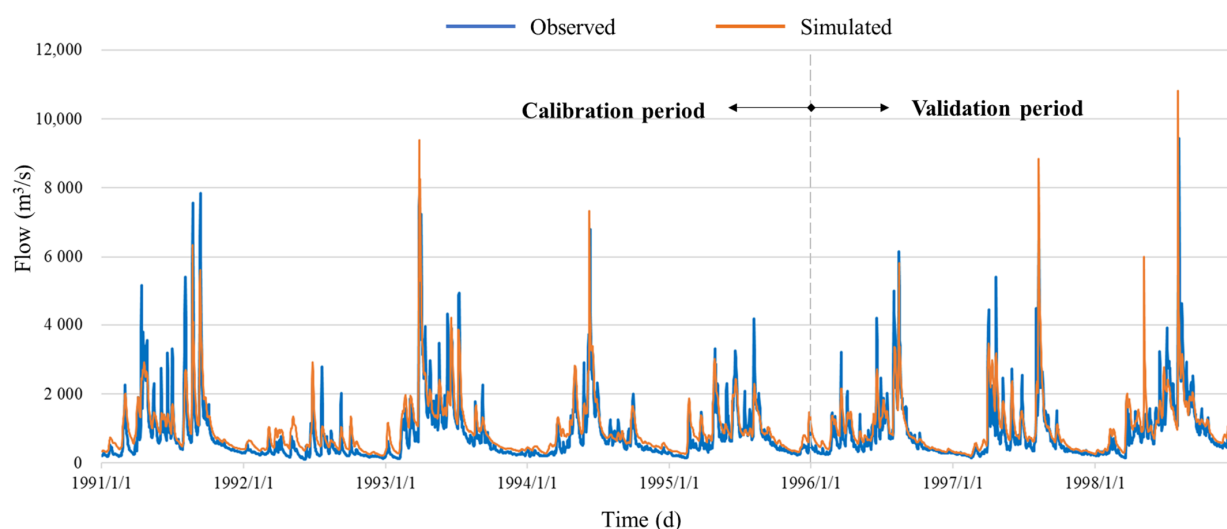

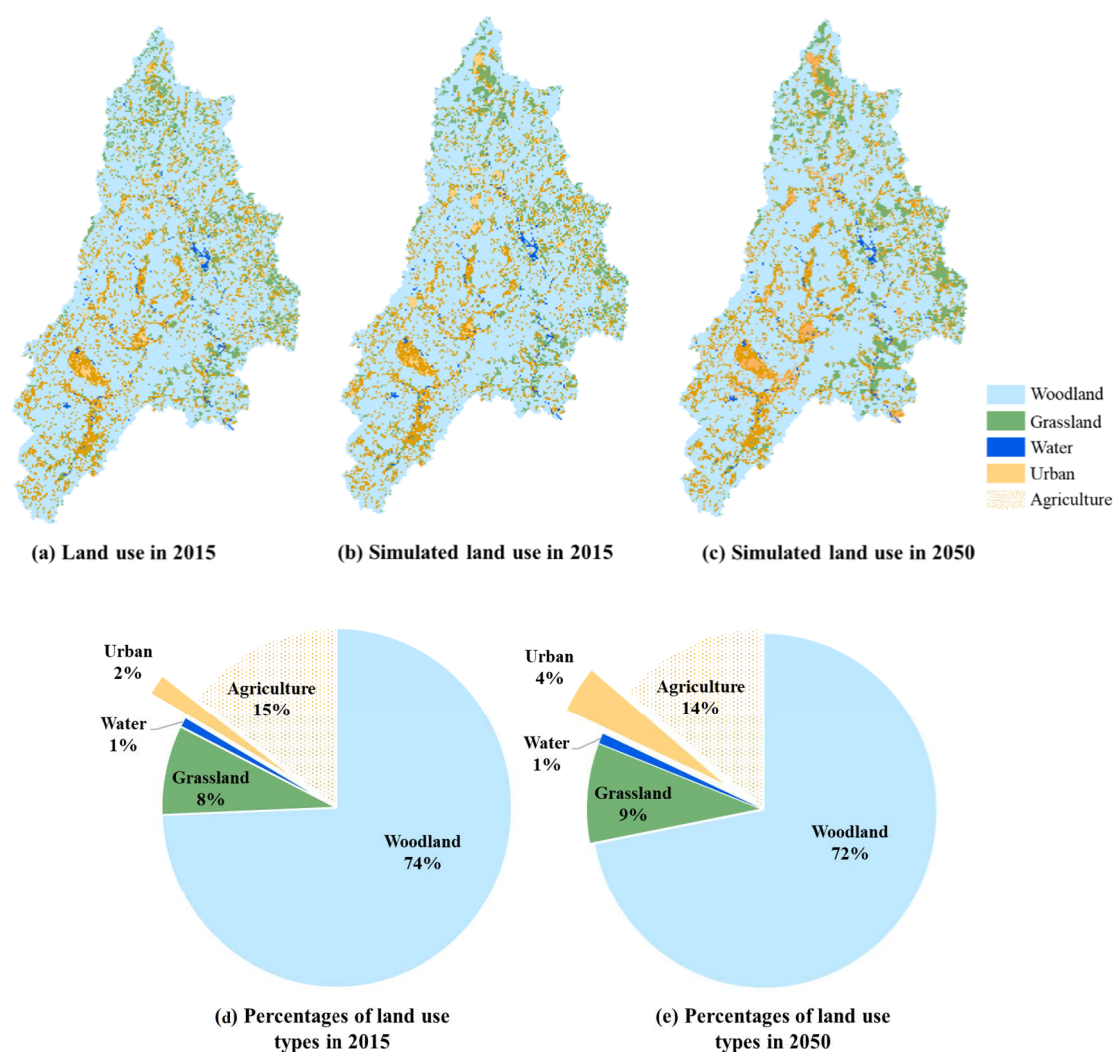**Figure 4.** Calibration and validation results of the SWAT model (1991~1998).

Table 2. Calibration and validation results of the SWAT model.

Period	NSE		RE (%)	R^2	
	Daily	**Monthly**		**Daily**	**Monthly**
Calibration	0.75	0.84	−7.53	0.74	0.84
Validation	0.71	0.87	9.70	0.73	0.92

4.2. Land Use and Land Cover

Figure 5a,b shows the real and the simulated land use maps in 2015. The Kappa index reaches up to 0.986, representing the reliability of the CA-Markov model.

The land use projection in 2050 shows that the area of the urban and grassland will continue to expand, from 2% and 8% to 4% and 9%, respectively. On the contrary, the area of woodland and agriculture will decrease from 74% and 15% to 71% and 14%, respectively. Among the four land use types, the relative change of urban area is relatively obvious, which expands from 691 to 1207 km^2, accounting for about 4% of the total area of Hanjiang River Basin above the Chaoan section. The most significant region where urban land expansion takes place is in the middle and upper reaches of the Meijiang River Basin. The population of this region reaches up to 3 million, about 40% of the total population of Hanjiang River Basin above the Chaoan section.

(a) Land use in 2015
(b) Simulated land use in 2015
(c) Simulated land use in 2050

Woodland
Grassland
Water
Urban
Agriculture

(d) Percentages of land use types in 2015
(e) Percentages of land use types in 2050

Figure 5. Simulation of land use patterns in the Hanjiang River Basin.

4.3. Hydrological Flow Regime Changes

Table 3 shows the flow regime changes at the Chaoan section under land use and climate changes. The land use changes will lead to a decline of Q_{90} and Q_{min7} by 1.8% and 0.6%, respectively, but an increase of $\overline{Q}$ and Q_{var} by 0.6% and 0.4%, respectively. The overall influence caused by land use changes is not large. As for the RCP 4.5 and 8.5 climate scenarios, $\overline{Q}$ will decrease by 2.3% and 5.2%, respectively; Q_{90} will decrease by 7.5% and 11.9%, respectively; Q_{min7} will increase by 1.3% and 0.7%, respectively; and Q_{var} will decrease by 3.9% and 6.3%, respectively. It shows that climate changes will lead to overall decreases of average flow and low flows in Hanjiang River Basin, and the variability of low flows will decrease, as well. Compared with the RCP 4.5 scenario, the flow will be drier under the RCP 8.5 scenario. Furthermore, the impact of climate changes on the streamflow in the Hanjiang River Basin will be higher than the land use changes, which makes the change pattern of low flows under the combined scenarios similar to the pattern under climate change only.

Table 3. Changes of low flow at the Chaoan cross section under changing environments.

Characteristics		Current (m³/s)	lu2050 (%)	rcp45 (%)	rcp85 (%)	rcp45_lu2050 (%)	rcp85_lu2050 (%)
Magnitude	Q_{90}	225.2	−1.8	−7.5	−11.9	−8.4	−12.5
	Q_{min7}	49.0	−0.6	+1.3	+0.7	+2.1	+1.4
	$\overline{Q}$	852.0	+0.6	−2.3	−5.2	−1.5	−4.4
Variability	Q_{var}	414.0	+0.4	−3.9	−6.3	−3.2	−5.4

Note: Lu2050 refers to the land use scenario for the year 2050; rcp45 and rcp85 refer to the RCP 4.5 and 8.5 climate scenarios, respectively. The shaded area indicates the negative value.

Figure 6 shows the flow duration curves and relative changes of the flows above the 50th percentile. To help visualize the flow data, especially low flow data, a logarithmic scale for the vertical axis is used in the flow duration curve (Figure 6a,b). The impact pattern of land use and climate changes on the flows in the 50th and 90th range is basically consistent. The absolute changes of flow between each projected scenario and the baseline scenario from Q_{50} to Q_{90} show a decreasing amplitude. Figure 6c shows that the relative changes of flow in the Q_{50}–Q_{75} range is relatively stable, while that in the Q_{75}–Q_{90} range becomes larger with the decrease of flow data. For the low flow over Q_{90}, the relative changes are still lower than the Q_{50}–Q_{75} range, even though there are some fluctuations. Therefore, the low flow is more sensitive to the changing environments.

The changes of streamflow for each month at the Chaoan section under changing environments are shown in Figure 7. The land use changes will amplify the flow during February and September, while reducing the flow in the rest of the months, but the overall influence is within ±2%. Compared with the land use change scenarios, climate changes will have a more significant impact on the monthly flow at the Chaoan section, with overall relative changes ranging from −33% to 21%. The flow will be amplified during June and August, while reduced in the rest of the months. For the two climate change scenarios, the flow will be lower under the RCP 8.5 scenario both in the flood season and dry season. The most severe flow decrease will appear before the flood season (February, March, and April), during which the maximum decrease amplitude will reach up to 32.3%. For the combined effect of land use and climate changes, the change amplitude will be larger in the flood season, while smaller in the dry season.
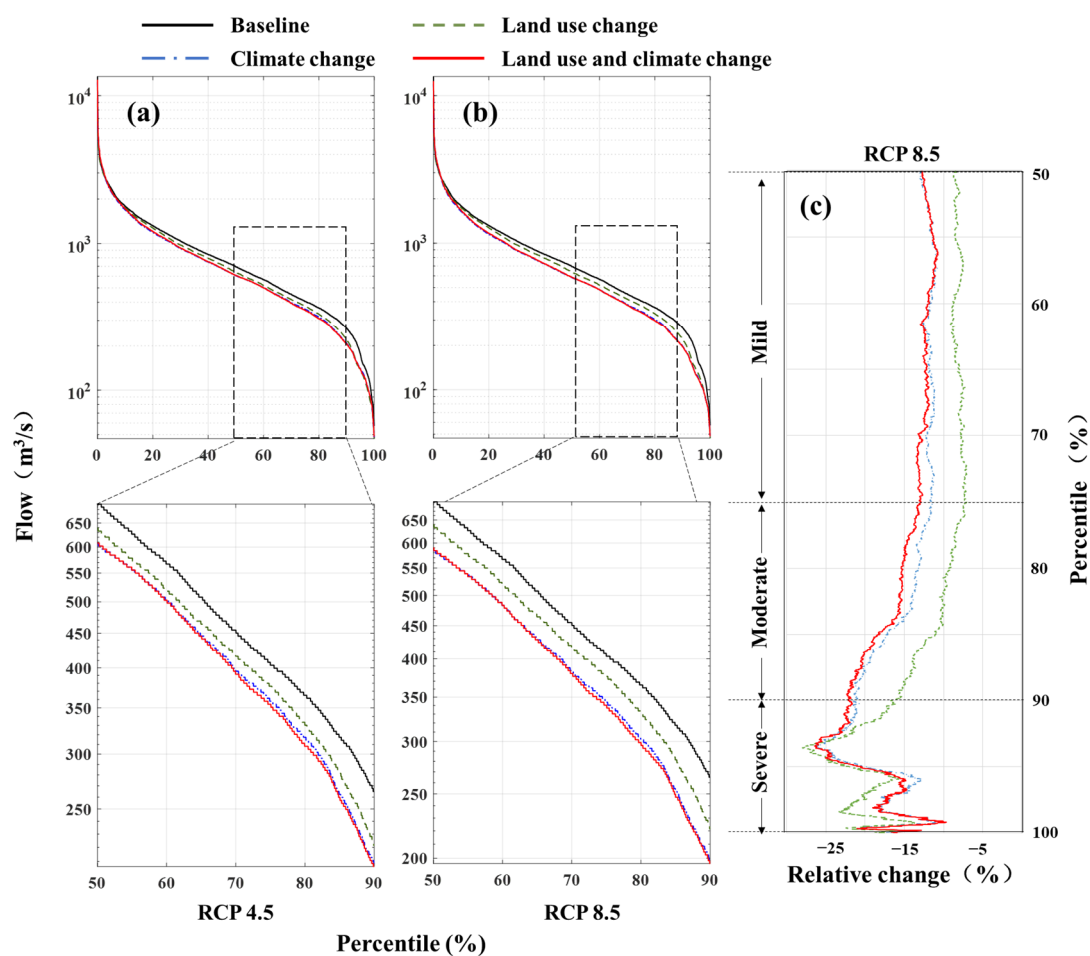
Figure 6. Logarithmic flow duration curves and relative changes of the flow at the Chaoan cross section.
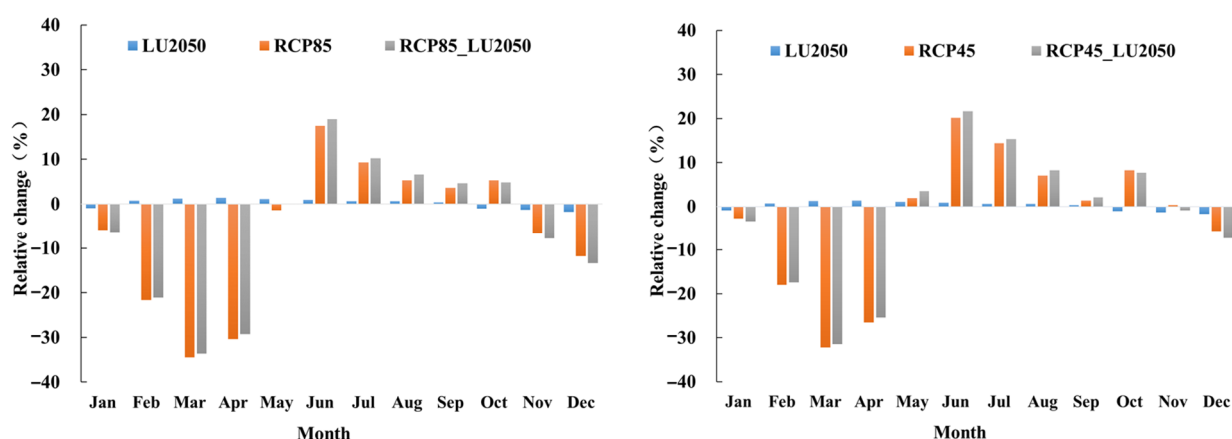

Figure 7. Changes of monthly flow at the Chaoan section under changing environments.

4.4. Assessment of Hedging Rules under Future Scenarios

Future flow regime projections indicate a severe decline of low flows in the dry season, especially from February to March. Moreover, a similar situation will appear in April. This indicates that the extension of water supply time and the increase of the water supply amount would bring more challenges on the water supply systems in the Hanjiang River Basin.

As the accumulated effects of different land use and climate change scenarios (i.e., RCP 4.5 and 8.5) are similar, RCP 8.5 combined with the LU2050 scenario was selected to evaluate the performance of hedging rules, since it would lead to relatively more severe drought conditions.

Figure 8 shows the Pareto solutions of water supply reliability and maximum water deficit, obtained by PA-DDS for HRs, in comparison with the solution of SOPs. The solution of COs is (61.6, 92.3), which is outside the axis ranges. Therefore, it has not been plotted. Both the solutions of HRs and SOPs are superior to the COs, suggesting that the joint operation of multiple reservoirs can make better use of water resources. Compared with the objectives of all the Pareto solutions using HRs, the SOPs have a close water supply reliability but relatively larger maximum water deficit depth. The Pareto front of HRs indicates that the increase of water supply reliability generally accompanies the increase of maximum water deficit depth, as they are two conflicting objectives in a water supply system with limited water resources.
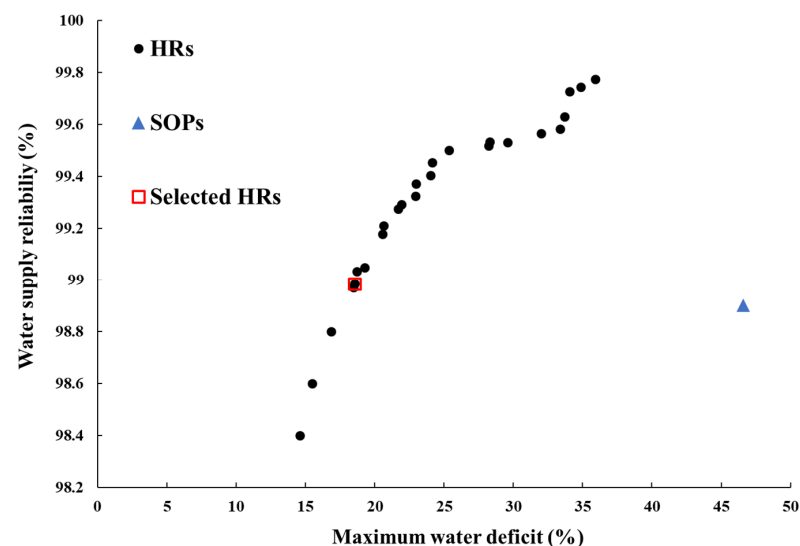

Figure 8. Pareto solutions of PA-DDS for HRs in comparison with the SOPs solution.

Considering the trade-off between the two objectives, it would be better to select a set of operation rules which can guarantee as much higher water supply reliability as possible on the premise of maximum water deficit within 20%. Therefore, the HRs with a solution of (18.54, 98.98), as shown in Figure 8, were selected. The selected HRs for the aggregated virtual reservoir and GB reservoir for each month are shown in Figures 9 and 10, respectively.

The performance of different operation rules under future scenarios (RCP8.5-LU2050) are shown in Figure 11. Results show that the I_{RS} obtained by the selected HRs is higher than either SOPs or COs, which indicates that the water supply system operating with HRs can be more quickly recovered in case of a severe water deficit period. The I_{RE} for HRs is close to that of SOPs, which is decided by the HRs selection in Figure 6, and improves by 7% compared with COs. The I_{VU} for the HRs is the lowest among the three reservoir operating rules, representing that HRs can help reduce the average water deficit. Moreover, the results show that the water supply system guided by SOPs is more vulnerable to future drought than the COs, even though SOPs improve the resiliency and reliability. This is likely due to the fact that SOPs give priority to ensure the water demand in the facing period, while that may lead to severe water deficit in the later period. Additionally, the I_S of HRs shows a preferable result compared with SOPs and COs. Therefore, it can be concluded that a reservoir operation system that is applied with HRs stably outperforms SOPs or COs in terms of resiliency, reliability, vulnerability, and sustainability.
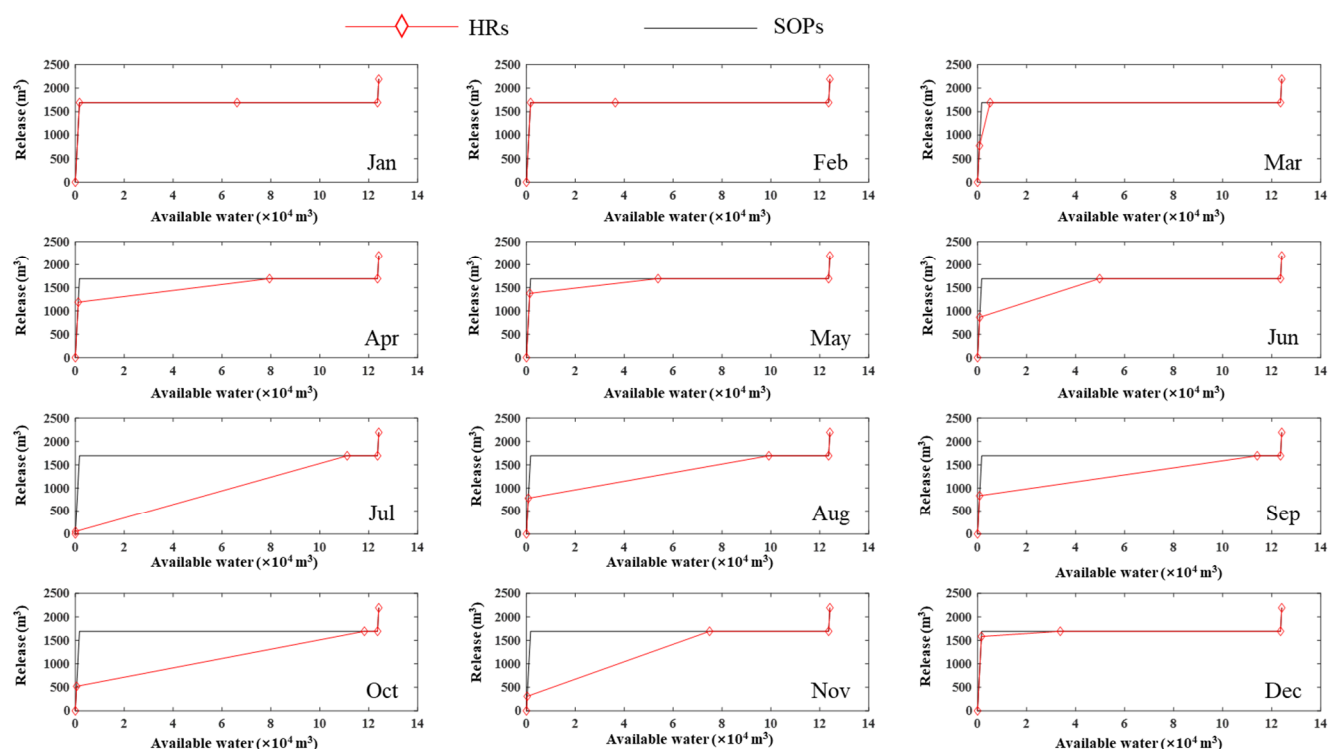
Figure 9. Selected HRs for the aggregated virtual reservoir for each month under future scenarios (RCP8.5-LU2050).
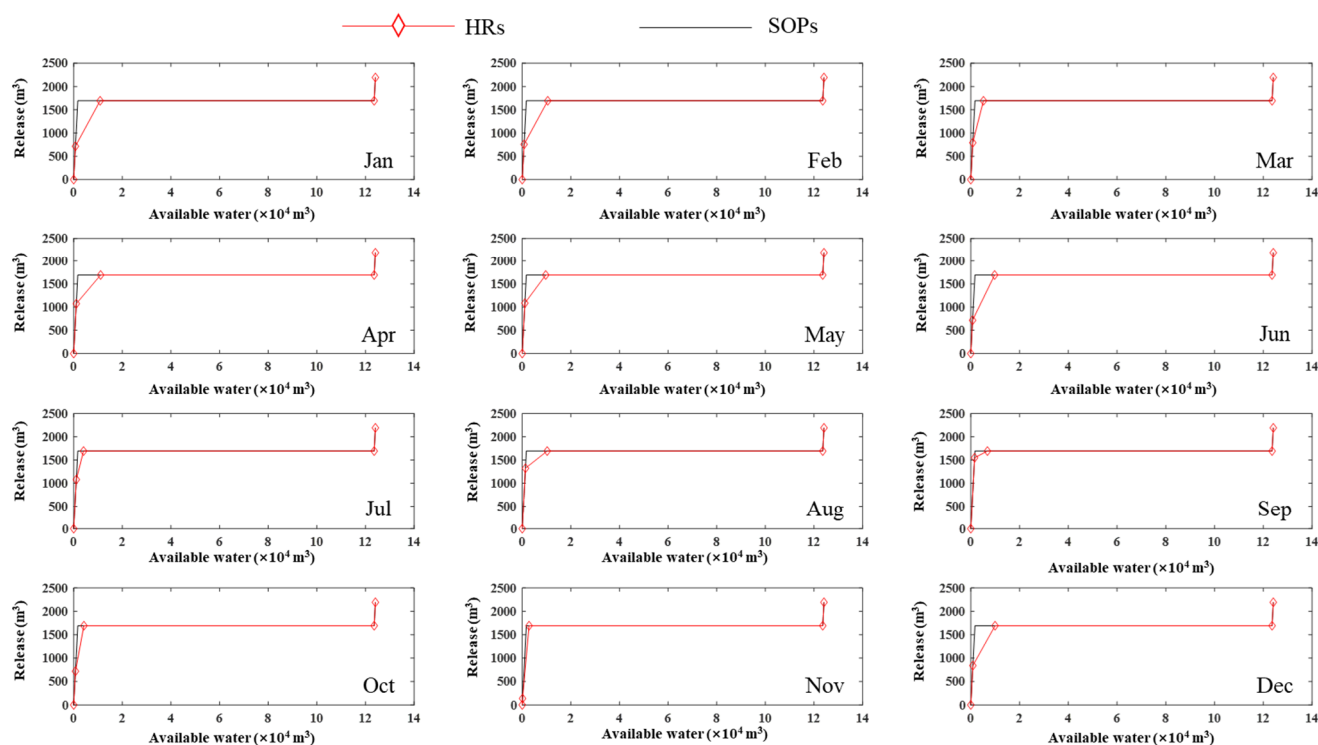

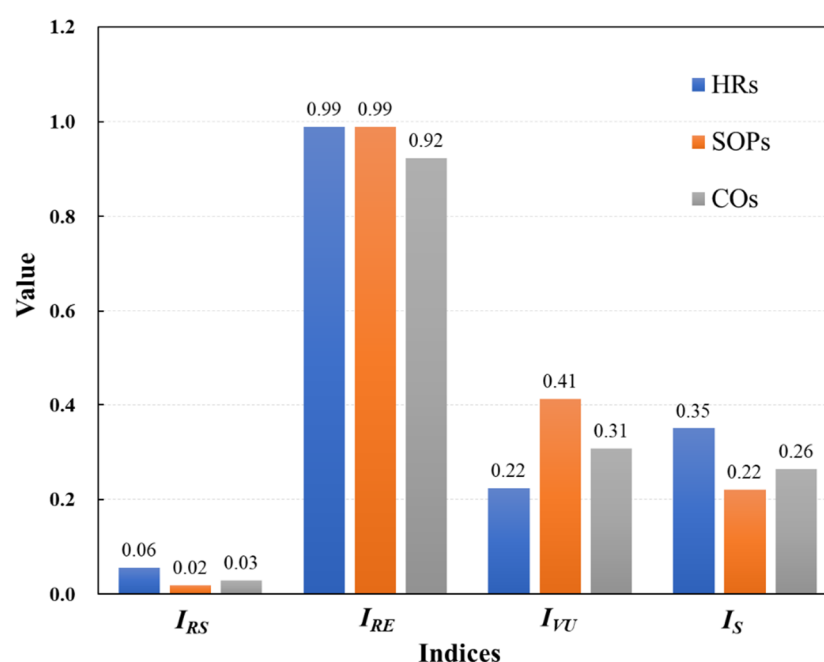**Figure 10.** Selected HRs for GB reservoir for each month under future scenarios (RCP8.5-LU2050).

Figure 11. Performance of different operation rules under future scenarios (RCP8.5-LU2050). I_{RS}–resilience, I_{RE}–reliability, I_{UV}–vulnerability, I_S–sustainability.

4.5. Discussion

This study investigated possible adaptive strategies for the multi-reservoir system under changing environments, and found the significant improved performance using the hedging rules, which was helpful for water resources management. However, there are still some aspects that need to be discussed.

(1.) On the changing environments

In this study, the land use change projection was conducted by the CA-Markov model. The model outputs depend on the initial state, which was the land use pattern in 2015, as well as the Markov transition matrix, which was calculated based on the land use map in 1995 and 2010. This makes the land use change projection a pure mathematical study. In reality, the change rate of land use in the Hanjiang River Basin may not remain the same for over 30 years. Land use will be affected by the changes in the population size and distribution, as well as the planning and management of local governments.

On the other hand, this study used the ensemble mean values of precipitation and air temperature to represent climate change projections in order to reduce the uncertainties of the GCM models. In fact, a better way to cope with future uncertainty could be to evaluate each climate scenario and determine the operation interval for the reservoirs by means of Bayesian model averaging or other methods.

In addition, it has to be pointed out that this study did not consider the change of anthropogenic water demands, which varies with population, agriculture, and industry. This should be considered in the future studies.

(2.) On the joint operation of multi-reservoir system

This study utilized the aggregation-decomposition method to guide the multi-reservoir operation, implying that all of the reservoirs can be managed by the same authority. In reality, four large reservoirs in the Hanjiang River Basin are located in two provinces (MHT in the Fujian province and the rest in the Guangdong province). This makes an ideal cooperative reservoir operation mode hard to achieve. A better approach to realize sustainable transboundary water governance could be to propose cooperative and self-enforcing alternatives to facilitate equitable water distribution [45].

(3.)   On the reservoir operating rules

This study applied the HRs into the reservoir operation. HRs can be regarded as an improvement on the basis of SOPs, which are one of the simplest and most widely used operating rules in water supply systems [46]. Nevertheless, adaptive strategies can be achieved in countless other ways, such as the optimization of operating rules in other forms [23,40,47] or the optimization of operating rule curves (Zhou et al., 2013). The performance of different adaptive strategies may vary with the structure of the reservoir network, the characteristics of the streamflow, and the water demand [48].

5. Conclusions

This study conducted the hydrologic simulation under climate and land use changes, and then derived the adaptive reservoir operating rules based on the hedging mechanism, in order to mitigate the possible damages of future drought conditions to the water supply system.

The SWAT hydrologic model was constructed for the Hanjiang River Basin. The CA-Markov model was utilized to generate land use projections in 2050. The Delta method was used to generate precipitation and temperature data under future climate scenarios including RCP 4.5 and 8.5. The separate and combined impact of land use changes and climate changes on low flows were investigated. Considering the limited water regulation capacity of the reservoirs in the Hanjiang River Basin, the hedging mechanism was introduced in the reservoir operating rules. Moreover, to guide the multi-reservoir operation, the aggregation-decomposition method was used. Four parallel reservoirs, which are MHT, CT, HS, and YT were aggregated into a virtual reservoir. To improve the water supply reliability and reduce the water deficit, a multi-objective optimization algorithm called PA-DDS was used to derive the optimal reservoir operating rules. The performance of HRs was compared with SOPs and COs. Two main conclusions could be drawn as follows:

(1.)   Hanjiang River Basin is expected to experience more severe drought conditions under the land use and climate changes. Lower flows are more sensitive to environmental changes and a decline of monthly flows can reach up to nearly 30% in the dry season.

(2.)   By applying HRs into the multi-reservoir operation in the Hanjiang River Basin, the water supply system can be more adaptive to the environmental changes in terms of reliability, resiliency, vulnerability, and sustainability, compared with SOPs and COs.

References

1. Li, J.; Wang, Z.; Wu, X.; Zscheischler, J.; Guo, S.; Chen, X. A standardized index for assessing sub-monthly compound dry and hot conditions with application in China. *Hydrol. Earth Syst. Sci.* **2021**, *25*, 1587–1601. [CrossRef]
2. Middelkoop, H.; Daamen, K.; Gellens, D.; Grabs, W.; Kwadijk, J.; Lang, H.; Parmet, B.W.A.H.; Schädler, B.; Schulla, J.; Wilke, K. Impact of Climate Change on Hydrological Regimes and Water Resources Management in the Rhine Basin. *Clim. Chang.* **2001**, *49*, 105–128. [CrossRef]
3. Xu, Y.-P.; Zhang, X.; Ran, Q.; Tian, Y. Impact of climate change on hydrology of upper reaches of Qiantang River Basin, East China. *J. Hydrol.* **2013**, *483*, 51–60. [CrossRef]
4. Cuo, L.; Lettenmaier, D.P.; Mattheussen, B.V.; Storck, P.; Wiley, M. Hydrologic prediction for urban watersheds with the Distributed Hydrology-Soil-Vegetation Model. *Hydrol. Process.* **2008**, *22*, 4205–4213. [CrossRef]
5. Nie, W.; Yuan, Y.; Kepner, W.; Nash, M.S.; Jackson, M.; Erickson, C. Assessing impacts of Landuse and Landcover changes on hydrology for the upper San Pedro watershed. *J. Hydrol.* **2011**, *407*, 105–114. [CrossRef]
6. Liu, Y.; Zhang, X.; Xia, D.; You, J.; Rong, Y.; Bakir, M. Impacts of land-use and climate changes on hydrologic processes in the Qingyi river watershed, China. *J. Hydrol. Eng.* **2013**, *18*, 1495–1512. [CrossRef]
7. Wang, G.; Yang, H.; Wang, L.; Xu, Z.; Xue, B. Using the SWAT model to assess impacts of land use changes on runoff generation in headwaters. *Hydrol. Process.* **2012**, *28*, 1032–1042. [CrossRef]
8. Li, J.; Wang, Z.; Wu, X.; Xu, C.-Y.; Guo, S.; Chen, X. Toward Monitoring Short-Term Droughts Using a Novel Daily Scale, Standardized Antecedent Precipitation Evapotranspiration Index. *J. Hydrometeorol.* **2020**, *21*, 891–908. [CrossRef]
9. Yang, P.; Ng, T.L. Fuzzy Inference System for Robust Rule-Based Reservoir Operation under Nonstationary Inflows. *J. Water Resour. Plan. Manag.* **2017**, *143*, 04016084. [CrossRef]
10. Biemans, H.; Haddeland, I.; Kabat, P.; Ludwig, F.; Hutjes, R.W.A.; Heinke, J.; Von Bloh, W.; Gerten, D. Impact of reservoirs on river discharge and irrigation water supply during the 20th century. *Water Resour. Res.* **2011**, *47*, W03509. [CrossRef]
11. Chen, J.; Shi, H.; Sivakumar, B.; Peart, M.R. Population, water, food, energy and dams. *Renew. Sustain. Energy Rev.* **2016**, *56*, 18–28. [CrossRef]
12. Mehran, A.; Mazdiyasni, O.; AghaKouchak, A. A hybrid framework for assessing socioeconomic drought: Linking climate variability, local resilience, and demand. *J. Geophys. Res. Atmos.* **2015**, *120*, 7520–7533. [CrossRef]
13. Xu, W.; Zhao, J.; Zhao, T.; Wang, Z. Adaptive Reservoir Operation Model Incorporating Nonstationary Inflow Prediction. *J. Water Resour. Plan. Manag.* **2015**, *141*, 04014099. [CrossRef]
14. Zhang, J.; Cai, X.; Lei, X.; Liu, P.; Wang, H. Real-time reservoir flood control operation enhanced by data assimilation. *J. Hydrol.* **2021**, *598*, 126426. [CrossRef]
15. Georgakakos, A.P.; Yao, H.; Kistenmacher, M.; Georgakakos, K.P.; Graham, N.E.; Cheng, F.Y.; Spencer, C.; Shamir, E. Value of adaptive water resources management in Northern California under climatic variability and change: Reservoir management. *J. Hydrol.* **2012**, *412–413*, 34–46. [CrossRef]
16. Bhaduri, A.; Bogardi, J.; Siddiqi, A.; Voigt, H.; Vörösmarty, C.; Pahl-Wostl, C.; Bunn, S.E.; Shrivastava, P.; Lawford, R.; Foster, S.; et al. Achieving Sustainable Development Goals from a Water Perspective. *Front. Environ. Sci.* **2016**, *4*, 64. [CrossRef]
17. Shiau, J.T.; Lee, H.C. Derivation of optimal hedging rules for a water-supply reservoir through compromise programming. *Water Resour. Manag.* **2005**, *19*, 111–132. [CrossRef]
18. Shih, J.; Revelle, C. Water-Supply Operations during Drought: Continuous Hedging Rule. *J. Water Resour. Plan. Manag.* **1994**, *120*, 613–629. [CrossRef]
19. You, J.-Y.; Cai, X. Hedging rule for reservoir operations: 1. A theoretical analysis. *Water Resour. Res.* **2008**, *44*, W01415. [CrossRef]
20. Steinschneider, S.; Brown, C. Dynamic reservoir management with real-option risk hedging as a robust adaptation to nonstationary climate. *Water Resour. Res.* **2012**, *48*, W05524. [CrossRef]
21. Karamouz, M.; Imen, S.; Nazif, S. Development of a Demand Driven Hydro-climatic Model for Drought Planning. *Water Resour. Manag.* **2011**, *26*, 329–357. [CrossRef]
22. Adeloye, A.J.; Soundharajan, B.-S. Effect of reservoir zones and hedging factor dynamism on reservoir adaptive capacity for climate change impacts. *Proc. Int. Assoc. Hydrol. Sci.* **2018**, *379*, 21–29. [CrossRef]
23. Alimohammadi, H.; Massah Bavani, A.R.; Roozbahani, A. Mitigating the impacts of climate change on the performance of multi-purpose reservoirs by changing the operation policy from SOP to MLDR. *Water Resour. Manage.* **2020**, *34*, 1495–1516. [CrossRef]
24. Ahmadianfar, I.; Zamani, R. Assessment of the hedging policy on reservoir operation for future drought conditions under climate change. *Clim. Chang.* **2020**, *159*, 253–268. [CrossRef]
25. Lei, X.; Zhang, J.; Wang, H.; Wang, M.; Khu, S.-T.; Li, Z.; Tan, Q. Deriving mixed reservoir operating rules for flood control based on weighted non-dominated sorting genetic algorithm II. *J. Hydrol.* **2018**, *564*, 967–983. [CrossRef]
26. Oliveira, R.; Loucks, D.P. Operating rules for multireservoir systems. *Water Resour. Res.* **1997**, *33*, 839–852. [CrossRef]
27. Zhang, J.; Wang, X.; Liu, P.; Lei, X.; Li, Z.; Gong, W.; Duan, Q.; Wang, H. Assessing the weighted multi-objective adaptive surrogate model optimization to derive large-scale reservoir operating rules with sensitivity analysis. *J. Hydrol.* **2016**, *544*, 613–627. [CrossRef]
28. Saad, M.; Turgeon, A.; Bigras, P.; Duquette, R. Learning disaggregation technique for the operation of long-term hydroelectric power systems. *Water Resour. Res.* **1994**, *30*, 3195–3202. [CrossRef]

29. Zhang, J.; Li, Z.; Wang, X.; Lei, X.; Liu, P.; Feng, M.; Khu, S.-T.; Wang, H. A novel method for deriving reservoir operating rules based on flood classification-aggregation-decomposition. *J. Hydrol.* **2018**, *568*, 722–734. [CrossRef]

30. Arnold, J.G.; Srinivasan, R.; Muttiah, R.S.; Williams, J.R. Large area hydrologic modeling and assessment part i: Model development. *Jawra J. Am. Water Resour. Assoc.* **1998**, *34*, 73–89. [CrossRef]

31. Li, Z.; Liu, P.; Feng, M.; Cui, X.; He, P.; Wang, C.; Zhang, J. Evaluating the Effect of Transpiration in Hydrologic Model Simulation through Parameter Calibration. *J. Hydrol. Eng.* **2020**, *25*, 04020007. [CrossRef]

32. Li, Z.; Liu, P.; Deng, C.; Guo, S.; He, P.; Wang, C. Evaluation of Estimation of Distribution Algorithm to Calibrate Computationally Intensive Hydrologic Model. *J. Hydrol. Eng.* **2016**, *21*, 04016012. [CrossRef]

33. Abbaspour, K.C.; Yang, J.; Maximov, I.; Siber, R.; Bogner, K.; Mieleitner, J.; Zobrist, J.; Srinivasan, R. Modelling hydrology and water quality in the pre-alpine/alpine Thur watershed using SWAT. *J. Hydrol.* **2007**, *333*, 413–430. [CrossRef]

34. Sang, L.; Zhang, C.; Yang, J.; Zhu, D.; Yun, W. Simulation of land use spatial pattern of towns and villages based on CA–Markov model. *Math. Comput. Model.* **2010**, *54*, 938–943. [CrossRef]

35. Dang, A.N.; Kawasaki, A. Integrating biophysical and socio-economic factors for land-use and land-cover change projection in agricultural economic regions. *Ecol. Model.* **2017**, *344*, 29–37. [CrossRef]

36. Navarro-Racines, C.E.; Tarapues, J.; Thornton, P.; Jarvis, A.; Ramirez-Villegas, J. High-resolution and bias-corrected CMIP5 projections for climate change impact assessments. *Sci. Data* **2020**, *7*, 1–14. [CrossRef] [PubMed]

37. Räty, O.; Räisänen, J.; Ylhäisi, J.S. Evaluation of delta change and bias correction methods for future daily precipitation: Intermodel cross-validation using ENSEMBLES simulations. *Clim. Dyn.* **2014**, *42*, 2287–2303. [CrossRef]

38. Asadzadeh, M.; Tolson, B. Pareto archived dynamically dimensioned search with hypervolume-based selection for multi-objective optimization. *Eng. Optim.* **2013**, *45*, 1489–1509. [CrossRef]

39. Asadzadeh, M.; Tolson, B.A.; Burn, D.H. A new selection metric for multiobjective hydrologic model calibration. *Water Resour. Res.* **2014**, *50*, 7082–7099. [CrossRef]

40. He, S.; Guo, S.; Yang, G.; Chen, K.; Liu, D.; Zhou, Y. Optimizing Operation Rules of Cascade Reservoirs for Adapting Climate Change. *Water Resour. Manag.* **2019**, *34*, 101–120. [CrossRef]

41. Yang, G.; Guo, S.; Liu, P.; Li, L.; Xu, C.-Y. Multiobjective reservoir operating rules based on cascade reservoir input variable selection method. *Water Resour. Res.* **2017**, *53*, 3446–3463. [CrossRef]

42. Thompson, J.R.; Laizé, C.L.R.; Green, A.J.; Acreman, M.C.; Kingston, D.G. Climate change uncertainty in environmental flows for the Mekong River. *Hydrol. Sci. J.* **2014**, *59*, 935–954. [CrossRef]

43. Asefa, T.; Clayton, J.; Adams, A.; Anderson, D. Performance evaluation of a water resources system under varying climatic conditions: Reliability, Resilience, Vulnerability and beyond. *J. Hydrol.* **2013**, *508*, 53–65. [CrossRef]

44. Kjeldsen, T.R.; Rosbjerg, D. Choice of reliability, resilience and vulnerability estimators for risk assessments of water resources system. *Hydrol. Sci. J.* **2004**, *49*, 767. [CrossRef]

45. Qin, J.; Fu, X.; Peng, S.; Xu, Y.; Huang, J.; Huang, S. Asymmetric Bargaining Model for Water Resource Allocation over Transboundary Rivers. *Int. J. Environ. Res. Public Health* **2019**, *16*, 1733. [CrossRef]

46. Bayazit, M.; Ünal, N.E. Effects of hedging on reservoir performance. *Water Resour. Res.* **1990**, *26*, 713–719. [CrossRef]

47. Ahmadi, M.; Haddad, O.B.; Loáiciga, H.A. Adaptive Reservoir Operation Rules under Climatic Change. *Water Resour. Manag.* **2014**, *29*, 1247–1266. [CrossRef]

48. Zhou, Y.; Guo, S. Incorporating ecological requirement into multipurpose reservoir operating rule curves for adaptation to climate change. *J. Hydrol.* **2013**, *498*, 153–164. [CrossRef]